A New Soft-Switched ZCZVT-PWM DC-DC Boost Converter

Yakup SAHIN[*1], Naim Suleyman TING[2]

[1]Bitlis Eren University, Engineering Faculty, Electrical Electronics Engineering Department, 13000, Bitlis
[2]Erzincan University, Engineering Faculty, Electrical Electronics Engineering Department, 24100, Erzincan

Abstract: In this paper, a new soft-switched zero-current transition and zero-voltage transition (ZCZVT) converter is proposed for family pulse width modulation (PWM) DC-DC converters. The proposed new converter assures the main switch turning on under zero-voltage transition and turning off under zero-current transition. The proposed new converter also decreases electromagnetic interference noises and operates under soft switching in a wide input voltage range. There is no additional voltage or current stress on the main devices. The proposed converter has low cost and simple control and structure. The theoretical analysis of the converter is clarified and the operating intervals are given in detail. The experimental results of the converter are obtained by a prototype with 500 W and 100 kHz. The overall efficiency of the proposed converter is 98.5% at nominal output power.

Yeni Bir Yumuşak Anahtarlamalı SASGG-DGM DA-DA Yükseltici Dönüştürücü

Özet: Bu çalışmada darbe genişlik modülasyonlu (DGM) DA-DA dönüştürücüler için yeni bir sıfır akım geçişli sıfır gerilim geçişli (SASGG) yumuşak anahtarlamalı bir dönüştürücü sunulmuştur. Önerilen dönüştürücü ana anahtar için iletime girmede sıfır gerilimde geçiş ve kesime girmede sıfır akımda geçiş anahtarlama sağlar. Önerilen dönüştürücü elektromanyetik gürültüleri azalttığı gibi geniş bir giriş gerilim skalasında da çalışabilir. Ana elemanlarda hiç bir akım ya da gerilim stresi oluşmaz. Önerilen dönüştürücü düşük maliyet, basit yapı ve control kolaylığı gibi özelliklere sahiptir. Dönüştürücünün teorik analizler yapılmış ve çalışma aralıkları detaylı bir şekilde verilmiştir. Önerilen dönüştürücünün deneysel verilerileri 500 W ve 100 kHz çalışma koşulları altında elde edilmiştir. Dönüştürücünün tam yükteki verimi %98.5 olarak ölçülmüştür.

1. Introduction

Pulse width modulation (PWM) DC-DC converters are often used in industry due to their fast dynamic response, simple structure, low cost, and easy control [1]. High switching frequency is desired in DC-DC converters. When the switching frequency is increased, power density increases and the cost decreases since the sizes of the inductance, capacitor, and transformer decrease at high frequencies. However, the high switching frequency causes switching losses and electromagnetic interference (EMI) noises. These issues cause the decrease of the total efficiency and performance of the converter. Therefore, zero-voltage switching (ZVS) and zero-current switching (ZCS) techniques are improved in order to reduce switching losses. In the fundamental zero-voltage transition (ZVT) converter, the voltage

of the main switch falls to zero with an active snubber cell while the main switch is in the off state [2]. Then a control signal is applied to the gate of the main switch while its voltage is zero. Thus, the main switch turns on without loss under ZVT. The main diode turns off under ZCS and the auxiliary switch turns on under ZCS. The main transistor and the auxiliary transistor also turn off under hard switching (HS). Many studies have been done to overcome these problems [3–6].

In the fundamental zero-current transition (ZCT) converter, first the current of the main switch is dropped to zero with an active snubber cell while the main switch is in the on state [7]. The control signal of the main switch is removed while its current is zero, so the main switch turns off under ZCT. The main diode turns on under ZVS and the auxiliary

switch turns on under ZCS, but the main switch turns on under HS. The auxiliary switch and the main diode turn off under HS. The main diode has a high reverse recovery loss. Many studies have been made to overcome these problems in ZCT techniques [8–11]. Turning off without switching loss is possible because of ZCT while turning on without switching loss is possible because of ZVT. Many studies have been done to eliminate disadvantages in the ZVT and ZCT techniques. However, these studies have many drawbacks, including HS, high EMI, and current or voltage stress. The best solution to overcome these drawbacks is combining the ZCT and ZVT techniques. Many studies have been made on the subject of combining ZCT and ZVT (ZCZVT) [12–18].

Some disadvantages occur with several soft-switched converters in the literature. In [6], turning off the main switch is not soft switching (SS). In [14], the SS conditionals depend on the duty cycle. The SS is not provided under a 0.5 duty cycle and there is an additional current stress on the main switch. In [12], a magnetic coupled inductor is used in the ZVT-ZCT converter. It needs tight magnetic coupling or else additional losses and parasitic oscillations occur due to the leakage inductance. In [15], there is additional current stress on the main switch. In this case, the values of the semiconductor devices and the losses of the converter increase. In [16], there is additional current stress on the main switch. It leads to both additional conduct losses and cost increase. A new converter is proposed here in order to overcome all of these problems and the proposed new converter is compared to that of [16]. The comparative efficiency results are examined with efficiency graphics.

2. Features and Operating Intervals of the Converter

2.1. Features of the proposed converter

The proposed new ZCZVT PWM DC-DC boost converter is shown in Figure 1. In this converter, ZVT is provided by turning on and ZCT is provided by turning off for the main switch. The main diode turns on under ZVS and turns off under ZCS. Additional current or voltage stress does not occur on the main switch and the main diode. The auxiliary switch and the auxiliary diode both turn on and turn off under ZCS. The proposed converter decreases EMI noise and operates even under a wide range of line and load voltages.

The features of the proposed ZCZVT-PWM boost converter can be summarized as follows:
➢ The main switch turns on with ZVT and turns off with ZCT. The main diode turns on with ZVS and turns off with ZCS. The auxiliary switch turns on and turns off with ZCS. Additionally, the other auxiliary semiconductor elements operate under soft switching.

➢ The extra current or voltage stress does not occur on the main switch.
➢ The extra current or voltage stress does not occur on the main diode.
➢ The proposed converter operates with soft switching for the overall line and load ranges. The snubber cell assures ZVT turn on and ZCT turn off under the light loads.
➢ The converter continues normal PWM operation in high frequencies.
➢ The transient intervals compose a small part of the period and the circulation energy is very low.
➢ The control of the converter is easy since the auxiliary and main switches are a common ground.
➢ This converter includes both ZVT and ZCT techniques in a cell using quite a few elements; because of that, it is cheap and simple compared to previous studies.
➢ The proposed converter can be easily applied to the other DC-DC converters.
➢ The snubber cell does not need extra passive elements.
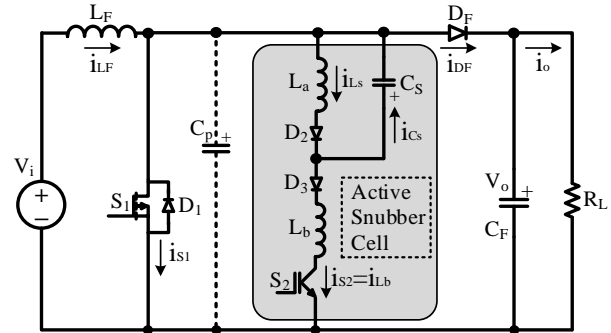
Figure 1. The basic circuit scheme of the proposed new ZCZVT-PWM DC-DC boost converter.

2.2. Operating intervals

Eleven intervals occur in the steady-state operation of the converter in one switching period. The equivalent circuits of these intervals are shown in Figure 2. The key waveforms of the operation intervals are shown in Figure 3.

Interval 1 [$t_0 < t < t_1$: Figure 2a]: Before t = t_0, the main switch S_1 and the auxiliary switch S_2 are in the off state. The main diode D_F conducts the input current I_i. At t = t_0, i_{S1} = 0, i_{DF} = I_i, i_{S2} = i L_b = 0, i L_a = 0, v C_p = V_o, and v_{Cs} = –V_{C0} are valid. At the beginning of this interval, a control signal is applied to auxiliary switch S_2 and the current of the main diode D_F decreases while the current of the auxiliary switch S_2 and the voltage of the snubber capacitor C_s increase. The main diode current $i_{DF}(t)$, lower resonant inductor current $i_{Lb}(t)$, and resonant capacitor voltage $v_{Cs}(t)$ can be expressed as follows:

$$i_{DF} = I_i - I_{Lb} = I_i - \frac{V_o + V_{C0}}{\omega_1 L_b} \sin\left(\omega_1\left(t - t_0\right)\right) \qquad (1)$$

$$i_{Lb} = \frac{V_o + V_{C0}}{\omega_1 L_b} \sin\left(\omega_1 \left(t - t_0\right)\right) \tag{2}$$

$$v_{Cs} = V_{C0} \cos\left(\omega_1 \left(t - t_0\right)\right) \tag{3}$$

where

$$\omega_1 = \sqrt{\frac{1}{L_b C_S}} \tag{4}$$

is valid. At $t = t_1$, the current of main diode D_F falls to zero when the current of the snubber inductance L_b reaches the input current I_i. The voltage of the snubber capacitor reaches a value of $(-V_{C1})$. Consequently, the auxiliary switch S_2 turns on under ZCS because of series resonance inductances L_b and the main diode D_F turns off under ZCS.

Interval 2 [$t_1 < t < t_2$: **Figure 2b**]: At $t = t_1$, $i_{S1} = 0$, $i_{DF} = 0$, $i_{S2} = i_{Lb} = I_i$, $i_{La} = 0$, $v_{Cp} = V_o$, and $v_{Cs} = -V_{C1}$ are valid. In this interval, a resonance begins between parasitic capacitor C_p and the snubber cell via C_p - C_s - L_b - S_2. The energy of C_p is transferred to the snubber cell. Thus, v_{Cp} voltage decreases while i_{Lb} current and v_{Cs} voltage are increasing. For this interval, the following equations are written:

$$i_{Lb} = I_i + \frac{V_o + V_{C1}}{\omega_2 L_b} \sin\left(\omega_2 \left(t - t_1\right)\right) \tag{5}$$

$$v_{Cp} = \left(V_o + V_{C1}\right) \cos\left(\omega_2 \left(t - t_1\right)\right) - V_{C1} \tag{6}$$

where,

$$\omega_2 = \sqrt{\frac{1}{L_b C_p}} \tag{7}$$

In the end of this interval, at $t = t_2$, v_{Cp} voltage falls to zero and i_{Lb} current is maximum. The voltage of snubber capacitor C_s is equal to zero.

Interval 3 [$t_2 < t < t_4$: **Figure 2c**]: At $t = t_2$, $i_{S1} = (I_i \{ I_{Lb2})$, $i_{DF} = 0$, $i_{S2} = i_{Lb} = I_{Lb2}$, $i_{La} = 0$, $v_{Cp} = 0$, and $v_{Cs} = 0$ are valid. In this interval, a new resonance starts via L_b - L_a - C_s. At thebeginning of this interval, the D_1 diode turns on under ZVS and the energy of the resonance inductor L_b is transferred to L_a and C_s. It is called the ZVT interval where D_1 is in the on state. A control signal is applied to the main switch S_1 when its internal diode conducts. In this way, the main switch S_1 turns on as lossless with ZVT.
At $t = t_3$, the current of snubber inductance L_b falls to the input current level and the D_1 diode turns off under ZCS. Then the current of the main switch increases and the current of snubber inductance L_b continues to decrease. For this interval, the following equations are written:

$$i_{La} = \frac{L_e}{L_a} I_{Lb2} \left(1 - \cos\left(\omega_3 \left(t - t_2\right)\right)\right) \tag{8}$$

$$i_{Lb} = \frac{V_o + V_{C0}}{\omega_1 L_b} \sin\left(\omega_1 \left(t - t_0\right)\right) \tag{9}$$

$$v_{Cs} = V_{C0} \cos\left(\omega_1 \left(t - t_0\right)\right) \tag{10}$$
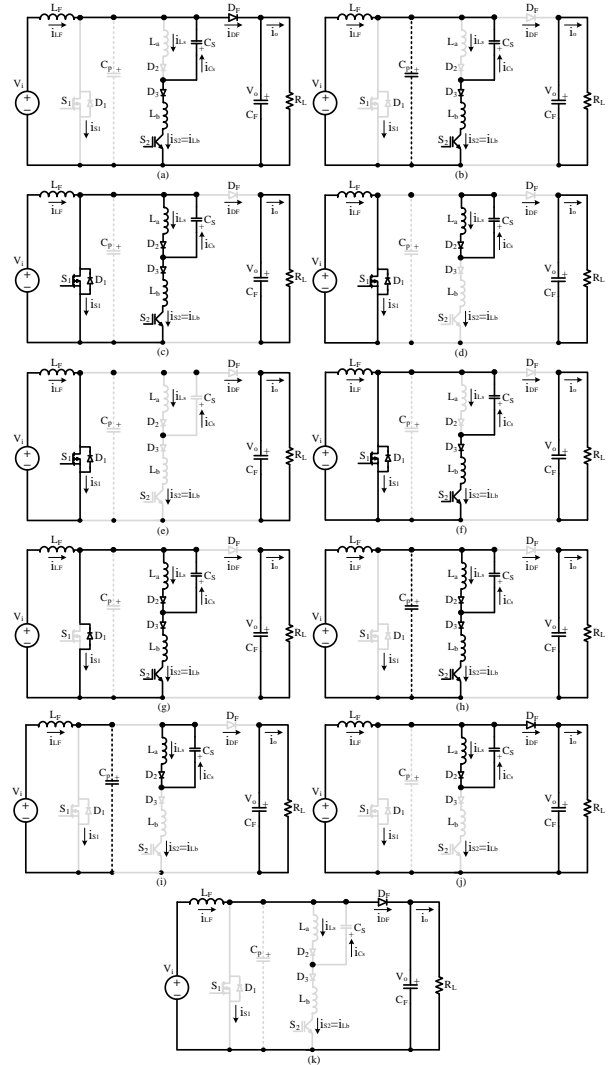
Figure 2. Equivalent circuit schemes of the operating intervals in the proposed ZCZVT-PWM DC-DC boost converter.

where

$$L_e = \frac{L_a L_b}{L_a + L_b} \tag{11}$$

$$\omega_3 = \sqrt{\frac{1}{L_e C_S}} \tag{12}$$

$$Z_1 = \sqrt{\frac{L_e}{C_S}} \tag{13}$$

At t = t_4, the current of snubber inductance L_b falls to zero when the current of main switch S_1 reaches the input current value and this interval is finished.

Interval 4 [$t_4 < t < t_5$: **Figure 2d**]: At t = t_4, i_{S1} = I_i, i_{DF} = 0, i_{S2} = i_{Lb} = 0, i_{La} = I_{La4}, v_{Cp} = 0, and v_{Cs} = V_{C4} are valid. At the beginning of this interval, after the current of S_1 reaches the input current value, auxiliary switch S_2 must be turned off under ZCS because the current of S_2 falls to zero. During this interval, the energy stored in upper snubber inductance L_a is transferred to capacitor C_s via L_a - D_2 - C_s resonance. For this interval, the following equations are written:

$$L_e = \frac{L_a L_b}{L_a + L_b} \tag{14}$$

$$\omega_3 = \sqrt{\frac{1}{L_e C_S}} \tag{15}$$

where,

$$Z_1 = \sqrt{\frac{L_e}{C_S}} \tag{16}$$

$$\omega_4 = \sqrt{\frac{1}{L_a C_S}} \tag{17}$$

$$v_{Cs\,max} = \sqrt{V_{C4}^2 + \left(Z_2 I_{La4}\right)^2} \tag{18}$$

At t = t_5, the voltage of capacitor C_s reaches the maximum voltage value in the adverse direction and the current of snubber inductor L_a falls to zero. This interval is then finished.

Interval 5 [$t_5 < t < t_6$: **Figure 2e**]: During this interval of the conventional boost converter, the main switch S_1 conducts the input current I_i. At t = t_6, a control signal is applied to the main switch S_1 and this interval is finished.

Interval 6 [$t_6 < t < t_8$: **Figure 2f**]: At t = t_6, i_{S1} = I_i, i_{DF} = 0, i_{S2} = i_{Lb} = 0, i_{La} = 0, v_{Cp}=0, and v_{Cs} = -V_{Csmax} are valid. At the beginning of this interval, a control signal is applied to auxiliary switch S_2 and it turns on under ZCS because of series snubber inductance L_b. A resonance starts between the snubber capacitor C_s and the snubber inductance L_b via C_s - L_b -S_2 - D_1. The current of the main switch S_1 begins to decrease while the current of snubber inductance L_b is increasing.

At t = t_7, the current of S_1 falls to zero when the current of L_b reaches the input current value. D_1 conducts the excess of input current. This interval is called the ZCT interval where D_1 is in the on state. The control signal of the main switch S_1 is removed

when its internal diode is in the on state. In this way, the main switch S_1 turns off as lossless under ZCT. At the same time, the resonance via C_s - L_b - S_2 - D_1 goes on. For this interval, the following equations are written:

$$i_{Lb} = i_{S2} = \frac{V_{Cs\,max}}{Z_3} \sin\left(\omega_1 \left(t - t_6\right)\right) \tag{19}$$

$$v_{Cs} = V_{Cs\,max} \cos\left(\omega_1 \left(t - t_6\right)\right) \tag{20}$$

where,

$$Z_3 = \sqrt{\frac{L_b}{C_S}} \tag{21}$$

$$i_{Lb\,max} = \frac{V_{Cs\,max}}{Z_3} \tag{22}$$

At t = t_8, the current of snubber inductance L_b reaches the maximum value (I_{Lbmax}) when the voltage of snubber capacitor C_s falls to zero. This interval is then finished.

Interval 7 [$t_8 < t < t_9$: **Figure 2g**]: At t = t_8, i_{S1} = (I_i - I_{Lbmax}) , i_{DF} = 0, i_{S2} = i_{Lb} = I_{Lbmax}, i_{La} = 0, v_{Cp} = 0, and v_{Cs} = 0 are valid.
In this interval, a new resonance starts via L_b - L_a - C_s. The energy of the resonance inductor L_b is transferred to L_a and C_s. Then the voltage of snubber capacitor C_s begins to become positive and the current of L_a begins to increase. For this interval, the following equations are written:

$$i_{La} = \frac{L_e}{L_a} I_{Lb\,max} \left(1 - \cos\left(\omega_3 \left(t - t_8\right)\right)\right) \tag{23}$$

$$i_{Lb} = \frac{L_e}{L_a} I_{Lb\,max} \left(1 - \cos\left(\omega_3 \left(t - t_8\right)\right)\right) + I_{Lb\,max} \left(1 - \cos\left(\omega_3 \left(t - t_8\right)\right)\right) \tag{24}$$

$$v_{Cs} = \frac{I_{Lb\,max}}{\omega_3 C_S} \sin\left(\omega_3 \left(t - t_8\right)\right) \tag{25}$$

At t = t_9, D1 turns off as soon as the current of L_b falls to the input current value and this interval is finished.

Interval 8 [$t_9 < t < t_{10}$: **Figure 2h**]: At t = t_9, i_{S1} = 0, i_{DF} = 0, i_{S2} = i_{Lb} = I_i, i_{La} = I_{L9}, v_{Cp} = 0, and v_{Cs} = V_{C9} are valid. This interval begins when D_1 turns off. Then a resonance occurs via C_p- L_a - L_b - C_s under the constant input current. During this interval, the current of L_a and the voltage of C_s increase while the current of snubber inductance L_b decreases. For this interval, the following equations are written:

$$L_a \frac{di_{La}}{dt} = v_{Cs} \tag{26}$$

$$L_b \frac{di_{Lb}}{dt} = v_{Cp} - v_{Cs} \qquad (27)$$

$$C_S \frac{dv_{Cs}}{dt} = i_{Lb} - i_{La} \qquad (28)$$

$$C_p \frac{dv_{Cp}}{dt} = I - i_{Lb} \qquad (29)$$

At t = t_{10}, the current of L_b falls to zero and the control signal of S_2 is removed, so S_2 turns off under ZCS and this interval is finished.
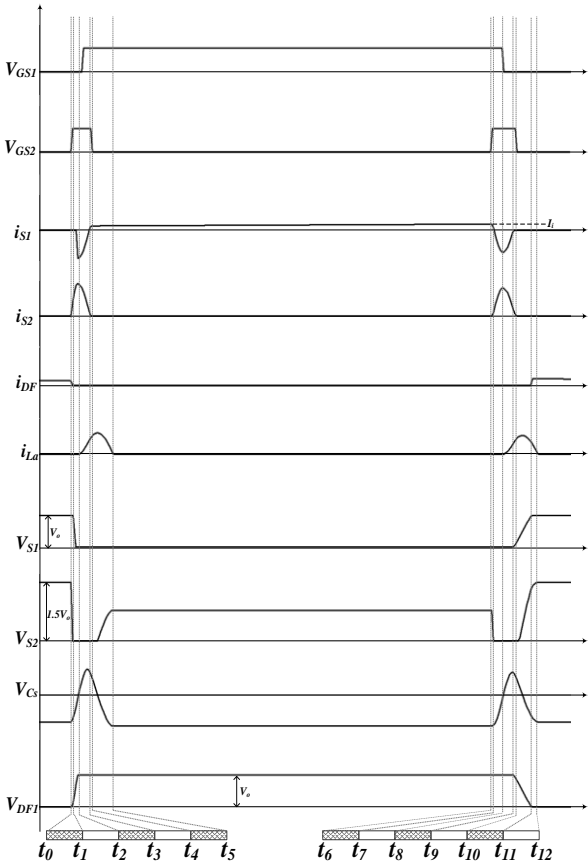
Figure 3. The key waveforms of the operation intervals of the proposed ZCZVT-PWM DC-DC boost converter.

Interval 9 [$t_{10} < t < t_{11}$: **Figure 2i**]: At t = t_{10}, i_{S1} = 0, i_{DF} = 0, $i_{S2} = i_{Lb}$ = 0, i_{La} = I_{L10}, v_{Cp} = V_{p10}, and v_{Cs} = V_{C10} are valid. In this interval, there are two different circuits. The parasitic capacitor C_p is linearly charged under the constant input current and the energy stored in the upper snubber inductance L_a is transferred to C_s via L_a - D_2 - C_s resonance. For this interval, the following equations are written:

$$i_{La} = I_{La10} \cos\left(\omega_4 (t-t_{10})\right) + \frac{V_{Cs10}}{Z_2} \sin\left(\omega_4 (t-t_{10})\right) \qquad (30)$$

$$v_{Cs} = V_{Cs10} \cos\left(\omega_4 (t-t_{10})\right) + Z_2 I_{La10} \sin\left(\omega_4 (t-t_{10})\right) \qquad (31)$$

$$v_{Cp} = \frac{I_i}{C_p}(t-t_{10}) \qquad (32)$$

At t = t_{11}, the main diode D_F turns on under ZVS as soon as the voltage of C_p is equal to the output voltage. Then this interval is finished.

Interval 10 [$t_{11} < t < t_{12}$: **Figure 2j**]: At t = t_{11}, i_{S1} = 0, i_{DF} = I_i, $i_{S2} = i_{Lb}$ = 0, i_{La} = I_{L11}, v_{Cp} = V_o, and v_{Cs} = $-V_{C11}$ are valid. In this interval, the resonance between L_a and C_s continues. All of the energy stored in the snubber inductance L_a is transferred to C_s. For this interval, the following equations are written:

$$i_{La} = I_{La11} \cos\left(\omega_4 (t-t_{11})\right) + \frac{V_{Cs11}}{Z_2} \sin\left(\omega_4 (t-t_{11})\right) \qquad (33)$$

$$v_{Cs} = -V_{Cs11} \cos\left(\omega_4 (t-t_{11})\right) + Z_2 I_{La11} \sin\left(\omega_4 (t-t_{11})\right) \qquad (34)$$

At t = t_{12}, the current of the snubber inductor L_a falls to zero and v_{Cs} voltage reaches to $-V_{C0}$ interval is finished.

Interval 11 [$t_{12} < t < t_{13} = t_0$: **Figure 2k**]: In this interval, in which the main diode D_F is in the on state, the input current is transferred to the output through D_F. This mode is the conventional PWM boost converter, which is in the off state interval. Thus, it is returned to initial conditions and the intervals expressed are repeated in the next switching cycle.

3. Design Procedure of Proposed Converter

The characteristic curves of the ZCZVT PWM DC-DC boost converter are shown in Figures 4{7. These curves will be considered when the elements of the converter are determined. In these curves, the value of snubber inductance L_b is kept constant at 3 H and the variations of L_a and C_s are graphically shown.

As shown in Figure 4, the duration of ZVT increases while the value of L_a is decreasing and the value of C_s is increasing. Figure 5 illustrates that the duration of ZCT is constant while the value of L_a is increasing. On the other hand, the duration of ZCT increases when the value of C_s increases.
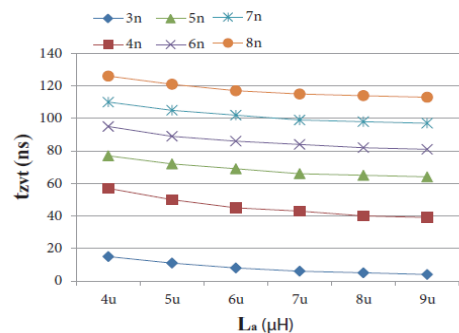
Figure 4. The variation of main switch ZVT duration

depending on L_a – C_S.
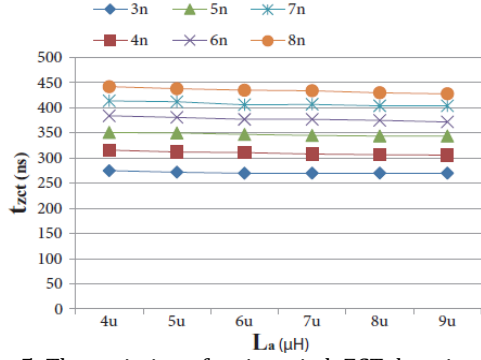
Figure 5. The variation of main switch ZCT duration depending on L_a– C_S.
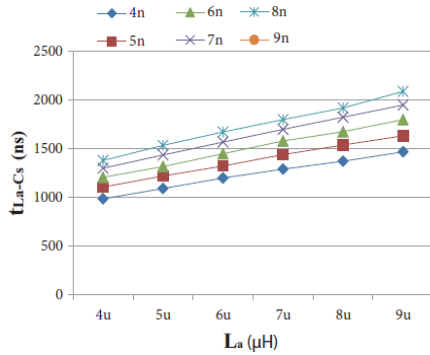
Figure 6. The variation of resonance duration between L_a– C_S.
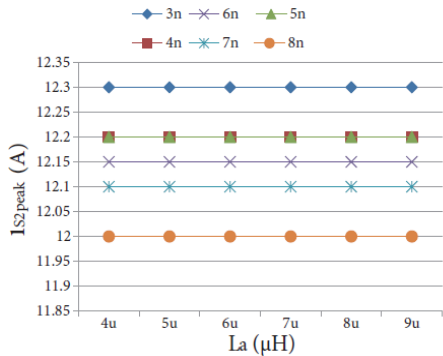
Figure 7. The variation of the auxiliary switch peak current depending on L_a - C_S.

In Figure 6, as expressed in the fourth interval, the variations of resonance duration between L_a and C_s are shown. This duration is more important because it affects the total time of resonance between interval 8 and interval 10. It is possible to see from the curves that $t_{La\ Cs}$ durations increase depending on the increasing of the values L_a and C_s.$t_{La\ Cs}$ is the resonance duration between L_a and C_s.

Finally, Figure 7 illustrates the variations of resonance peak current that the auxiliary switch S_2 conducts. This peak value is fairly important in order to provide ZVT and ZCT conditionals. It is shown from the curves that the variation of L_a does not change the peak current of S_2 but the decreasing of C_s is increasing the peak value of this current. As shown in the figure, the resonance current reaches a level of twice the input current.

1.   The parasitic capacitor C_p consists of the parasitic capacitor of the main switch and the other parasitic capacitors. This value is almost 1.2 nF. Therefore, it does not require an extra capacitor.
2.   The snubber inductance L_b must choose to provide ZCS turn on for auxiliary switch S_2. The turned on duration t_r of S_2 is considered while this value is being determined.

$$\frac{V_O}{L_b}t_r \leq I_{i\max} \qquad (35)$$

At the same time, the value of snubber inductance L_a should be at least twice as big as L_b because the auxiliary switch S_2 is turned off with ZCS.

$$L_a \geq 2L_b \qquad (36)$$

In this case, the value of snubber inductance L_b is chosen as 3µH and then L_a is 6µH.

As shown in Figures 4 and 5, a smaller snubber capacitor means shorter ZCT and ZVT durations. Shorter ZVT and ZCT durations are undesirable. If the value of C_s is increased, ZVT and ZCT durations increase. However, in this case, the resonance duration between L_a– C_S and the other resonance durations will be extended. Consequently, the transient resonance intervals increase in the period and an undesirable case occurs because the total transient resonance intervals should be less than 20% of the total time of a period in order to assure PWM operation. For this reason, the value of C_S cannot be increased over a determined value. Finally, the peak value of the resonance current should be twice the peak value of the main inductance current because the SS should ensure even in the worst conditions that the input current is the maximum value. Figure 7 can be used for determining this current value. It is seen that the most suitable value for C_S is 4.7 nF.

4. Experimental Results

The photograph of the experimental circuit is given in Figure 8. A prototype of the proposed ZCZVT PWM DC-DC boost converter with 500 W and 100 kHz was realized at the laboratory. The nominal values of elements used in the converter are shown in Table 1 by considering datasheets of manufacturers.

Table 1. Nominal values of the semiconductors in the used experimental circuit.

Device	Part number	V (V)	I (A)	t_r(ns)	t_f(ns)	t_{rr}(ns)
S_1	IXGR50N60C2D1	600	40	45	40	140
S_2	BUP 203	1000	23	30	20	-
D_F	MUR860	600	8	-	-	60
D_2	DESI8-06	600	8	-	-	50
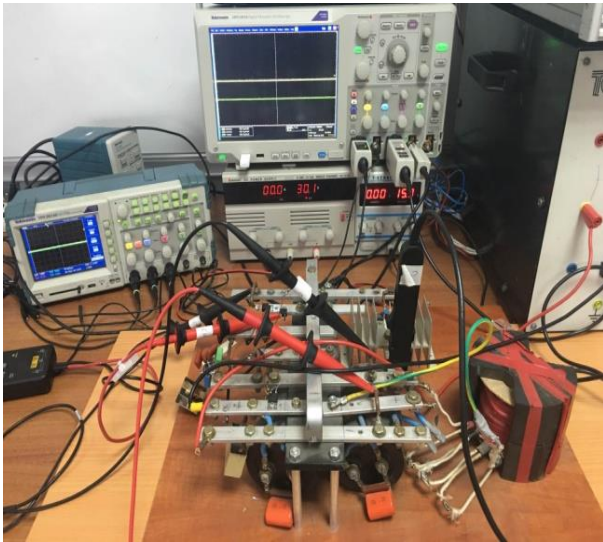
Figure 8. Photo of the experimental circuit.

Figure 9 shows the experimental results of the proposed new ZCZVT-PWM DC-DC boost converter taken at full load. These results verify the previously mentioned theoretical analysis. In Figure 9a, the control signals of the auxiliary and the main switch are shown. The auxiliary switch operates twice in one switching cycle of the main switch.

In Figure 9b, the control signal and the current of the main switch are shown. As shown in the figure, the control signal is applied and removed while the body diode of the main switch is in the on status, so ZVT and ZCT are perfectly assured.

In Figure 9c, the current and the voltage waveforms of the main switch are shown. As shown in the gure, the voltage of the main switch falls to zero with the snubber cell before the main switch is turned on. Then the main switch turns on under ZVT while the body diode of the main switch conducts. Likewise, the current of the main switch falls to zero with the snubber cell before the main switch turns off.

Then the main switch turns off under ZCT while the body diode of the main switch conducts. It is seen that there is not any voltage or current stress on the main switch. In Figure 9d, the current and the voltage waveforms of the main diode obtained from experimental results are given. As shown in the Figure, the main diode turns on under ZVS and turns off under ZCS. It seems that there is not any voltage or current stress on the main diode. In Figure 9e, the current and voltage waveforms of the auxiliary switch are shown. As shown in the Figure, the auxiliary switch turns on and turns off under ZCS.
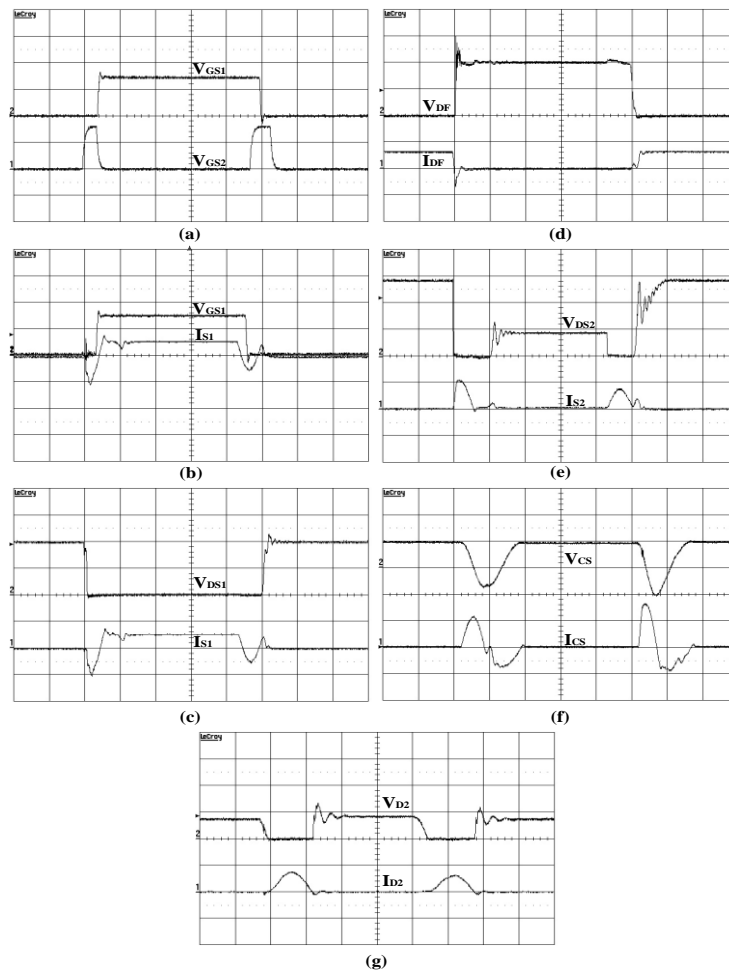
Figure 9. Experimental results: (a) control signals of S_1 and S_2 (10 V/div and 1 s/div); (b) control signal of S_1 and current of S_1 (10 V/div, 5 A/div, and 1 s/div); voltages and currents of (c) S_1 , (d) D_F , (e) S_2 , (f) C_s , (g) D_2 (200 V/div, 5 A/div, and 1 s/div).

Additionally, it is shown from the results that there is additional voltage stress on the auxiliary switch and its value is equal to 1.5 Vo. In Figures 9f and 9g, the voltage and current waveforms of C_s and D_2 are shown. As shown in the Figure, the voltages of C_s and D_2 do not exceed the output voltage.

The efficiency graphics of the new converter for SS and HS are shown in Figure 10. While the efficiency value of the converter is 92.8% under HS, it is measured at about 98.5% for SS at the nominal output power. Moreover, the soft-switched new converter is compared with the converter in [16] and it is shown in graphics that the efficiency of the new proposed converter is higher. The theoretical analysis of the new ZCZVT-PWM boost converter is verified with the experimental results.
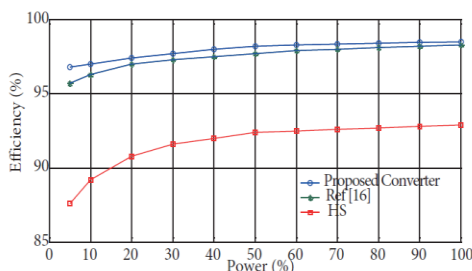
Figure 10. Efficiency graphics of the proposed new converter in the case of SS and HS.

5. Conclusions

In this paper, a new ZCZVT-PWM DC-DC boost converter with an active snubber cell is proposed. The proposed converter has advantages of the previous ZVT and ZCT studies and it also eliminates their disadvantages. The snubber cell of the proposed converter operates in a small part of the period and ensures that the main switch turns on ZVT and turns off ZCT in a lossless manner. Moreover, it ensures that the main diode turns on ZVS and turns off ZCS. Thus, it minimizes the reverse recovery losses of the main diode. It also does not add any extra voltage or current stress to the main devices. The current stress of the auxiliary switch is at an acceptable level. Considering all these features, an improved ZCZVT-PWM DC-DC converter that combines the advantages of PWM and resonance operating in a snubber cell and overcomes the disadvantages is proposed.

References

[1] Bodur, T., Bakan, A. F. 2002. A New ZVT-PWM DC–DC Converter. IEEE Transaction on Power Electronics, 17, 40-47.

[2] Hua, G.C., Leu, C. S., Jiang, Y. M., Lee, F. C. 1994. Novel Zero-voltage-Transition PWM Converters. IEEE Transaction on Power Electronics, 9, 213-219.

[3] Bodur, H., Cetin, S., Yanık, G. 2011. A New Zero Voltage Transition Pulse Width Modulated Boost Converter. IET Power Electronics, 4, 827-834.

[4] Jain, N., Jain, P. K., Joos, G. 2004. A Zero Voltage Transition Boost Converter Employing a Soft Switching Auxiliary Circuit with Reduced Conduction Losses. IEEE Transaction on Power Electronics, 29, 130-139.

[5] Gurunathan, R., Bhat, A. K. S. 2002. A Zero-Voltage Transition Boost Converter Using a Zero-Voltage Switching Auxiliary Circuit. IEEE Transaction on Power Electronics, 17, 658-668.

[6] Huang, W., Gao, X., Bassan, S., Moschopoulos, G. 2008. Novel dual auxiliary circuits for ZVT-PWM converter. Canadian Journal Electrical Computer Engineering, 33, 74-82.

[7] Hua, G. C., Yang, E. X., Jiang, Y. M., Lee, F. C. 1994. Novel Zero-Current-Transition PWM Converters. IEEE Transaction on Power Electro., 9, 601-606.

[8] Bodur, H., Bakan, A. F. 2004. An Improved ZCT-PWM DC–DC Converter for High-Power and Frequency Applications. IEEE Transaction Industrial Electronics, 51, 89-95.

[9] Adib, E., Farzanehfard, H. 2008. Family of Zero-Current Transition PWM Converters. IEEE Transactions on Industrial Electronics, 55, 3055-3063.

[10] Das, P., Moschopoulos, G. 2007. A Comparative Study of Zero-Current-Transition PWM Converters. IEEE Transactions on Industrial Electronics, 54, 1319-1328.

[11] Lee, D. Y., Lee, M. K., Hyun, D. S., Choy, I. 2003. New Zero-Current-Transition PWM DC/DC Converters without Current Stress. IEEE Transaction on Power Electronics, 18, 95-104.

[12] Molavi, N., Adib, E., Farzenahfard, H. 2018. Soft-switching bidirectional DC–DC converter with high voltage conversion ratio. IET Power Electronics, 11, 33-42.

[13] Sahin, Y., Ting, N. S., Aksoy, I. 2017. A highly Efficient ZVT-ZCT PWM Boost Converter with direct Power Transfer. Electrical Engineering, Doi: 10.1007/s00202-017-0546-y.

[14] Ting, N. S., Sahin, Y., Aksoy, I. 2017. Analysis, Design and Implementation of a Zero-Voltage-Transition Interleaved Boost Converter. Journal of Power Electronics, 17, 41-55.

[15] Ting, N. S., Aksoy, I., Sahin, Y. 2017. ZVT-PWM DC-DC Boost Converter with Active Snubber Cell. IET Power Electronics, 10, 251-260.

[16] Aksoy, I., Bodur, H., Bakan, A. F. 2010. A New ZVT-ZCT PWM DC-DC Converter. IEEE Transaction on Power Electronics,25,2093-2105

[17] Sahin, Y. 2018. A Novel Soft Switching PWM-PFC AC-DC Boost Converter. Journal of Electrical Engineering and Technology, 13, 256-262.

[18] Sahin, Y., Ting, N. S. 2018. A Soft Switching with Reduced Voltage Stress Zvt-Pwm Full-Bridge Converter, Review of Scientific Instruments, 89, 045105 - 1 - 045105 – 9.